Gold-Adatom-Mediated Bonding in Self-Assembled Short-Chain Alkanethiolate Species on the Au(111) Surface

Peter Maksymovych,[1] Dan C. Sorescu,[2] and John T. Yates, Jr.[1,*]

[1]*Surface Science Center, Department of Chemistry, University of Pittsburgh, Pittsburgh, Pennsylvania 15260, USA*
[2]*National Energy Technology Laboratory, U.S. Department of Energy, Pittsburgh, Pennsylvania 15236, USA*

(Received 17 May 2006; published 6 October 2006)

Microscopic evidence for Au-adatom-induced self-assembly of alkanethiolate species on the Au(111) surface is presented. Based on STM measurements and density-functional theory calculations, a new model for the low-coverage self-assembled monolayer of alkanethiolate on the Au(111) surface is developed, which involves the adsorbate complexes incorporating Au adatoms. It is also concluded that the Au(111) herringbone reconstruction is lifted by the alkanethiolate self-assembly because the reconstructed surface layer provides reactive Au adatoms that drive self-assembly.

DOI: 10.1103/PhysRevLett.97.146103 PACS numbers: 68.43.Fg, 68.37.Ef, 68.43.Hn

The majority of self-assembled molecular monolayers (SAMs) are currently grown using the adsorption of organosulfur compounds (thiols, *R*S-H, and dithiols, *R*S-S*R*) on the Au(111) surface [1]. The applications of thiol-based SAMs are very diverse, including molecular electronics, biorecognition, and nanotechnology (see Ref. [2], and references therein). Upon adsorption at elevated temperatures, the thiol or dithiol molecules dissociate, forming the thiolate species (*R*S), which is the molecular building block of the SAM. Despite some years of research in this field, the structural nature of the S-Au anchor bond of the *R*S species to the Au(111) surface is still a matter of active debate [3–5]. The anchor bond significantly influences the self-assembly process and the SAM structure as well as the electronic properties of the molecule in the self-assembled layer [6–8]. An understanding of the thiolate bonding is required to explain the morphological changes of the Au(111) surface that accompany molecular self-assembly, such as the lifting of the Au(111) herringbone reconstruction and production of etch pits [9,10].

Recent discussion of the *R*S-Au bonding has focused on the discrepancy between theoretical and experimental predictions of the adsorption site of the thiolate species on the Au(111) surface. In a series of spectroscopic studies [by near-incidence x-ray standing wave analysis (NIXSW) at low and high coverages [3] and by photoelectron diffraction (PD) at low [4] and high [5] coverages], the *R*S species made by thermal dissociation of *R*S-H molecules were shown to occupy singly coordinated atop surface sites. This is inconsistent with theoretical calculations for this system, which conclude that the twofold bridge or threefold hollow sites on the Au(111) surface will have the highest thiolate binding energy [11]. In order to resolve this issue, deficiencies of the theoretical methods [5], coverage effects [12], or surface reconstruction at elevated temperatures [3] were proposed. The latter possibility is particularly appealing, because there exist theoretical models of the reconstructed Au(111) surface in which the thiolate is predicted to bond on atop Au sites [13]. Adsorbate-induced reconstruction of the Au(111) surface involving Au adatoms was proposed only a few times based on indirect evidence [14,15] and very recently from a detailed NIXSW study of several alkanethiol-derived SAMs produced by thermal dissociation [16]. However, no direct *microscopic* evidence of adatom bonding of *R*S species exists so far, and the role of the Au adatoms in the self-assembly process is unknown.

Here we present the first microscopic evidence for the Au-adatom involvement in the bonding of the alkanethiolate species to the Au(111) surface. Based on the scanning tunneling microscopy (STM) study of prototypical CH_3SSCH_3, CH_3SH, and C_3H_7SH molecules, we have derived a new structural model for the stripe phase of alkanethiols on the Au(111) surface (lowest-coverage SAM [1]), which involves pairs of *R*S species bonded via a Au adatom (*R*S-Au-SR). The density-functional theory (DFT) calculations show that each *R*S species in the new model indeed forms a singly coordinated bond to the Au(111) surface, which resolves the controversy raised by the previous spectroscopic studies of the low-coverage stripe-phase SAM [3,4]. Furthermore, we show for the first time that the herringbone reconstructed surface acts as a source of reactive of gold adatoms driving thiolate self-assembly.

The experiments were conducted with a low temperature STM (Omicron) operating in an ultrahigh vacuum chamber (background pressure $< 5.0 \times 10^{-11}$ Torr). The Au(111) crystal was cleaned by Ar^+ sputtering and annealing to 773 K. CH_3SSCH_3, CH_3SH, and C_3H_7SH were purified using several freeze-pump-thaw cycles. Each molecule was deposited on the surface through an effusive beam doser while the crystal was in the STM imaging position at <10 K. If necessary, the surface was subsequently heated to higher temperatures, where molecular dissociation and self-assembly occur. All the STM images presented here were taken at a temperature of 5 K.

The DFT calculations were done on periodic slab models using VASP [17] with the PW91 generalized gradient approximation [18]. The electron-ion interaction was de-

scribed using the projector augmented wave method of Blöchl [19] in the implementation of Kresse and Joubert [20]. The plane-wave basis cutoff energy was 400 eV. A $2 \times 2 \times 1$ Monkhorst-Pack [21] grid of k points was used to sample the Brillouin zone. All of the calculations were done in a 4×2 slab model (along the $\langle 1\bar{1}0 \rangle$ and $\langle 11\bar{2} \rangle$ axes) with four Au layers. The bottom two layers of the slab were kept frozen at bulk optimized positions.

Figure 1 shows the STM images of three forms of CH_3SSCH_3 on the Au(111) surface—undissociated, as dosed at 10 K [Fig. 1(a)], dissociated at 5 K by tunneling electrons at 1.0 V [Fig. 1(b)], and thermally dissociated at 300 K [Figs. 1(c) and 1(d)]. Thermally produced CH_3S forms chains of distinct repeat units [Fig. 1(d)], and the areal profile of each unit is about twice as large as a single CH_3S species in Fig. 1(b). The chain structure is known as a stripe phase, and it represents a flat-lying self-assembled layer (with carbon chains of alkyl groups parallel to the surface), which is the precursor to high coverage SAM layers involving upright thiolate species [10]. The stripe-phase chains always grow in the $\langle 11\bar{2} \rangle$ azimuthal direction with a periodicity of ~0.47 nm between repeat units, which is consistent with previous reports [1,22,23].

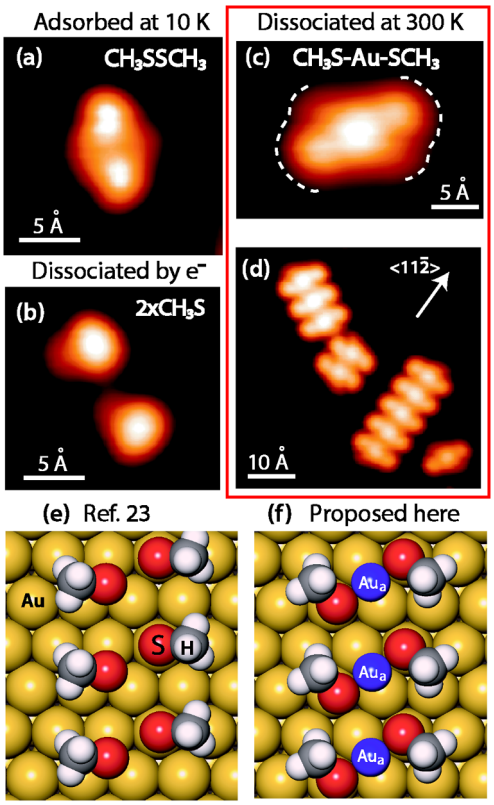

FIG. 1 (color online). STM images of the adsorbed molecular species studied. (a) A single CH_3S-SCH_3 molecule. (b) Two CH_3S fragments formed by pulsing CH_3S-SCH_3 with a 1.0 V pulse at 5 K. (c) Close-up of a single stripe-phase unit. The asymmetrical boundaries of the CH_3S species are marked by dashed white lines. (d) Chains of the CH_3S stripe phase after heating CH_3S-SCH_3 on Au(111) to 300 K. Top-view models of the CH_3S stripe phase according to (e) Ref. [23] and (c) proposed here (Au_a is the adatom).

In the current models of the stripe phase [4,23], the repeat unit is a pair of *RS* species, with headgroup-S atoms facing each other and forming a weak S-S bond [Fig. 1(e)]. We compared a single stripe-phase unit to chemisorbed CH_3SSCH_3 and CH_3S species, using the stability of molecules in STM imaging as a qualitative estimate of the relative binding strength.

The CH_3SSCH_3 molecule can be stably imaged only at a bias of less than 0.5 V. At higher voltages, CH_3SSCH_3 undergoes tip-induced motion, and the molecule dissociates above 1.0 V, producing (at 5 K) two CH_3S species bonded to the surface lattice. A single CH_3S species, despite its maximum calculated binding energy of ~40 kcal/mol on Au(111) [11], can be translated on the surface by applying pulses of 0.7–1.0 V at 1.0 nA. This is likely due to small potential barriers between neighbor CH_3S adsorption sites [11]. The imaging stability of the stripe-phase unit in Fig. 1(c) is starkly different from both adsorbed CH_3SSCH_3 and CH_3S, *as it is virtually indestructible by the tunneling current and voltage*. The unit can be imaged at voltages up to 4.5 V without diffusion or decomposition, and it can sustain large imaging currents up to 20 nA. This immense stability against high fields and currents cannot be explained by the structural model illustrated in Fig. 1(e).

We propose that the thermally produced thiolate is stabilized by Au adatoms as shown in Fig. 1(f). Metal adatoms form spontaneously on a number of metal surfaces at elevated temperatures. Adatom complexes with adsorbate molecules are known to have significantly higher binding energies, and this was also theoretically shown for the CH_3S species on the Au(111) surface [13].

Involvement of a Au adatom provides a straightforward explanation of the topographical appearance of the stripe-phase repeat unit. As seen in Fig. 1(c), high-resolution STM topography of the pair unit can be divided into two identical asymmetrical features, antiparallel to each other, separated by a single bright protrusion. Since there are two CH_3S fragments in the unit, each asymmetrical feature corresponds to a single CH_3S. Then the central protrusion can be assigned to the Au adatom. We have also verified that a similar central bright protrusion exists in the stripe phases derived from CH_3SH and from a longer alkanethiol C_3H_7SH. In the current stripe-phase model [Fig. 1(e)], the central feature corresponds to a pair of headgroup-S atoms and the CH_3 groups are on the periphery, which makes it difficult to explain the asymmetry of the peripheral features.

The new adatom-bonded structural model of the stripe-phase unit [Figs. 2(a) and 2(b)] was obtained using DFT calculations. In the input structure, the Au adatom was initially placed above a threefold hollow fcc site, and the two CH_3S fragments were symmetrically arranged on two

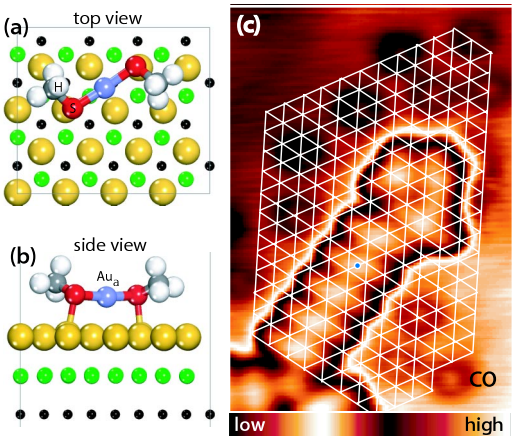

FIG. 2 (color online). Structure of CH_3S-Au-SCH_3 on Au(111). (a),(b) Calculated structure of the adatom-bonded pair unit which forms the CH_3S stripe phase. (c) Triangulation of the CH_3S stripe phase relative to the underlying lattice using CO molecules as markers of the Au lattice atoms. The off-hollow position of the Au adatom (blue circle) agrees well with the theoretical predictions presented in this work.

hollow sites around the adatom. Unexpectedly, the minimization process results in the shift of the Au adatom from the threefold hollow site to the twofold bridge site as shown in Figs. 2(a) and 2(b). At the same time, each CH_3S species assumes a new adsorption configuration, in which the headgroup-S atom of CH_3S makes one bond to the Au adatom and one bond to the underlying lattice atom giving r(S-Au-adatom) = 2.33 Å and r(S-Au-lattice) = 2.49 Å. The predicted off-hollow position of the Au adatom in the stripe-phase units is indeed observed by STM as seen in Fig. 2(c), where the blue dot indicates that the Au adatom is located on a bridge site above the surface plane. Here the surface Au lattice grid was determined using CO molecules as markers of lattice atoms. As expected, the presence of the Au adatom in the complex increases the binding energy of a single CH_3S species to 55.3 kcal/mol, compared to the 43.4 kcal/mol binding energy calculated for the most stable CH_3S configuration on the Au(111) surface. [The binding energy of the adatom-bonded CH_3S was determined relative to the gas phase CH_3S and the Au(111) surface with the Au adatom on the hollow fcc site.]

The new model of the stripe phase is in good agreement with recent NIXSW [3] and PD [3] studies, where it was found that the headgroup-S atom is adsorbed atop of a lattice Au atom forming a singly coordinated bond. Each S atom in our calculated model also makes one bond to the lattice Au atom and is located directly above this atom [Figs. 2(a) and 2(b)]. Moreover, the calculated bond length between the S atom and the lattice Au atom is 2.49 Å, which agrees well with the values reported for the stripe phases of long-chain alkanethiolates: 2.50 ± 0.05 Å measured by NIXSW for $C_8H_{17}S$ [3] and 2.40 ± 0.05 Å measured by PD for $C_6H_{13}S$ [4]. The spectroscopic signature of the Au adatom may also be observed, but the adatom-bonded model of the stripe phase was not tested in the analysis of the NIXSW [3] and PD [4] data.

Further support for the involvement of Au adatoms in the thiolate self-assembly comes from the observation of a quantitative correlation between the production of the stripe phase and the lifting of the Au(111) $22 \times \sqrt{3}$-herringbone reconstruction (the latter always occurs in thiolate self-assembly [9]). The herringbone reconstruction is formed by embedding one Au atom per 22 surface atoms into the bulk-terminated surface layer along the $\langle 1\bar{1}0 \rangle$ direction [24]. The measured area of the $22 \times \sqrt{3}$ unit cell in our atomically resolved images of the Au(111) surface is 2.8 nm^2, in good agreement with previously reported values [24]. Since there are two embedded Au atoms in the $22 \times \sqrt{3}$ unit cell, the surface density of the embedded Au atoms is 0.7 atoms/nm^2.

We determined the number of remaining embedded Au atoms in the herringbone reconstruction after it is partially lifted by the thiolate stripe phase. The $22 \times \sqrt{3}$ unit cell has one fcc- and one hcp-stacked lattice region along the $\langle 1\bar{1}0 \rangle$ direction, which are separated by two solitons (regions of faulted vertical stacking) [25]. The number of the remaining reconstructed unit cells (each involving two embedded Au atoms) was determined by measuring the total length of the unfaulted soliton lines (Fig. 3) in the STM image and dividing it by 0.47 nm, which is the measured periodicity of the $22 \times \sqrt{3}$ unit cell along the $\langle 11\bar{2} \rangle$ direction of the soliton. Surprisingly, we find that the number of newly formed repeat units of the stripe phase is equal to the number of embedded Au atoms which have disappeared during thiolate self-assembly. This is shown in Fig. 3(b), where a bar graph shows the distribution of the embedded Au atoms in the herringbone reconstruction and the complexed Au adatoms in the stripe phase as a function of the stripe-phase coverage. The total coverage of the Au atoms (embedded and complexed) remains nearly constant (~0.7 Au/nm^2) at low and intermediate coverages of the stripe phase. This conclusion is valid for the stripe phases obtained from all the molecules studied: CH_3SSCH_3, CH_3SH, and C_3H_7SH.

Such a correlation quantitatively supports our stripe-phase model, where each repeat unit contains one Au adatom. Furthermore, it suggests that the herringbone reconstruction can provide reactive Au adatoms by ejecting them locally where the stripe phase is formed. Although the mechanism of adatom ejection from the reconstruction is outside the scope of our discussion, it is widely known that the herringbone reconstruction involves the formation of a periodic array of dislocations, the elbow sites [24], which are likely to act as local sources of Au adatoms.

The above correlation begins to break down at a higher stripe-phase coverage, because the number of stripe-phase units exceeds the number of embedded atoms in the her-

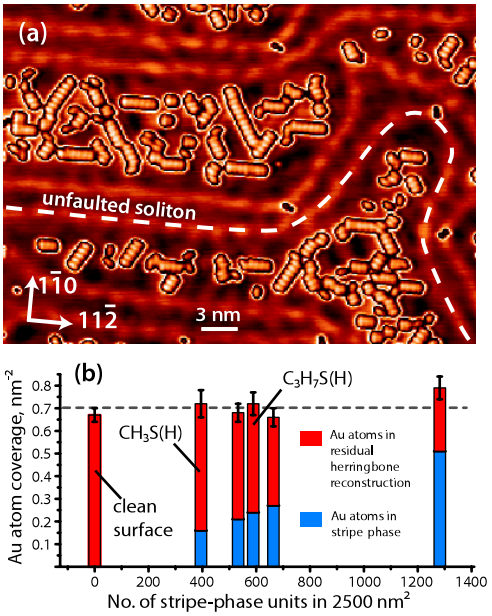

FIG. 3 (color online). Correlation between self-assembly of the stripe phase and lifting of the Au(111) herringbone reconstruction. (a) Typical large-scale sampling area of the Au(111) surface used for counting. The dashed line is the unfaulted soliton line. (b) Distribution of Au atoms (embedded herringbone atoms plus adatoms in the stripe phase) as a function of stripe-phase coverage for stripe phases produced from CH_3SSCH_3, CH_3SH (marked), and C_3H_7SH (marked).

ringbone reconstruction (at near saturation, stripe-phase unit density is as high as 1.2 nm^{-2}). In this case, random atomic steps, and ultimately the top bulk-terminated layer, become the source of Au adatoms, which is consistent with step-etching and etch-pit creation on the terraces that accompany thiolate self-assembly at high surface coverage [10].

The involvement of Au adatoms in initiating the thiolate self-assembly is also indicated by the similar temperatures needed for stripe-phase formation from *R*S-H and *R*S-S*R* molecules. Both CH_3SSCH_3 and CH_3SH dissociate to form the stripe phase near 200 K (this work and Refs. [6,26]). In all cases, the stripe phase is identical. The S-H bond in the gas phase CH_3SH is $\sim$1.0 eV stronger than the S-S bond in the gas phase CH_3SSCH_3 [27]. These facts can be consistently correlated by assuming that Au adatoms are involved in the breaking of the corresponding bonds and that Au-adatom creation is the limiting kinetic step for molecular dissociation and self-assembly at the low adsorbate coverages used in our experiments.

In summary, we have presented the first microscopic evidence for the adatom-mediated bonding in the self-assembly of alkanethiolate species on Au(111). The involvement of Au adatoms resolves the current controversy around the S-Au anchor bond in the low-coverage stripe-phase SAM and explains the morphological changes of the Au(111) surface, such as the lifting of the herringbone reconstruction. Although the involvement of the Au adatoms in the higher coverage 3D-self-assembled layers remains to be established, our results call upon a significant revision of the currently accepted mechanisms for the nucleation of the 2D stripe phase and the subsequent 2D to 3D transition of the SAM. The Au adatoms are also likely to influence the electronic properties of the molecules in the SAM. In addition, we anticipate that adatom-mediated chemistry on gold surfaces, and the role of the herringbone reconstruction as a source of chemically reactive Au adatoms, will have general implications for the field of heterogeneous catalysis and beyond.

We thank D. B. Dougherty for fruitful discussions. We thank the W. M. Keck Foundation for supporting this work. P. M. and J. T. Y., Jr. acknowledge NEDO (Japan) for financial support. A grant of computer time at the Pittsburgh Supercomputer Center is gratefully acknowledged.

*Corresponding author.
Electronic address: jyates@pitt.edu

[1] C. Vericat, M. E. Vela, and R. C. Salvarezza, Phys. Chem. Chem. Phys. **7**, 3258 (2005).
[2] J. C. Love *et al.*, Chem. Rev. **105**, 1103 (2005).
[3] M. G. Roper *et al.*, Chem. Phys. Lett. **389**, 87 (2004).
[4] T. Shimada *et al.*, Chem. Phys. Lett. **406**, 232 (2005).
[5] H. Kondoh *et al.*, Phys. Rev. Lett. **90**, 066102 (2003).
[6] V. De Renzi *et al.*, Phys. Rev. Lett. **95**, 046804 (2005).
[7] Q. Sun, A. Selloni, and G. Scoles, J. Phys. Chem. B **110**, 3493 (2006).
[8] Y. Xue and M. A. Ratner, Phys. Rev. B **69**, 085403 (2004).
[9] W. P. Fitts, J. M. White, and G. E. Poirier, Langmuir **18**, 1561 (2002).
[10] G. Poirier, Chem. Rev. **97**, 1117 (1997).
[11] Y. Yourdshahyan and A. M. Rappe, J. Chem. Phys. **117**, 825 (2002).
[12] X. Torrelles *et al.*, J. Phys. Chem. B **110**, 5586 (2006).
[13] L. M. Molina and B. Hammer, Chem. Phys. Lett. **360**, 264 (2002).
[14] S. J. Stranick *et al.*, J. Phys. Chem. **98**, 11 136 (1994).
[15] M. J. Esplandiu *et al.*, Surf. Sci. **600**, 155 (2006).
[16] D. P. Woodruff (private communication).
[17] G. Kresse and J. Hafner, Phys. Rev. B **48**, 13 115 (1993).
[18] J. P. Perdew and Y. Wang, Phys. Rev. B **45**, 13 244 (1992).
[19] P. E. Blöchl, Phys. Rev. B **50**, 17 953 (1994).
[20] G. Kresse and D. Joubert, Phys. Rev. B **59**, 1758 (1999).
[21] H. J. Monkhorst and J. D. Pack, Phys. Rev. B **13**, 5188 (1976).
[22] H. Kondoh *et al.*, J. Chem. Phys. **111**, 1175 (1999).
[23] R. Staub *et al.*, Langmuir **14**, 6693 (1998).
[24] J. V. Barth *et al.*, Phys. Rev. B **42**, 9307 (1990).
[25] U. Harten *et al.*, Phys. Rev. Lett. **54**, 2619 (1985).
[26] D. J. Lavrich *et al.*, J. Phys. Chem. B **102**, 3456 (1998).
[27] B. S. Jursic, Int. J. Quantum Chem. **62**, 291 (1997).